

Emergent failures and cascades in power grids: a statistical physics perspective

Tommaso Nesti and Bert Zwart
CWI, Amsterdam

Alessandro Zocca
California Institute of Technology

We consider complex networks where line failures occur indirectly as line flows are influenced by fluctuating input at nodes, a prime example being a power grid where power is generated by renewable sources. We examine the propagation of such emergent failures in the small noise regime, combining concepts from statistical physics and the physics of power flow. In particular we characterize rigorously and explicitly the configuration of inputs responsible for failures and cascades, and analyze the propagation of failures, which often is not of nearest-neighbor type.

Cascading failures in complex networks received a lot of attention in recent years [1–3, 10, 11, 13, 16–19, 26, 29–32]. Despite proposing different mechanisms for the cascade evolution, a common feature of all these works is that the cascade is assumed to be triggered by some *external* initiating event or contingency. This initial contingency, or *attack*, is chosen either (i) deliberately, e.g. targeting the most vulnerable or crucial network component, thus aiming for a worst-case analysis, or (ii) uniformly at random, in order to understand the average reliability of a network. This distinction led to the insight that complex networks are resilient to random attacks, but vulnerable to targeted attacks [8, 9, 19]. All attacks, random or deterministic, lead to *direct* failure of the target network line or node.

In the present work, we look at networks where line failures occur *indirectly*, by small fluctuations at the nodes. Our inspiration is drawn from the power grid [5, 12], and its potential vulnerability to fluctuations of renewable energy sources. Specifically, we look at the power grid as a static noise-perturbed system, where nodes are attacked *globally* but *indirectly* in the form of small fluctuations in the power injections. Due to the interplay between network structure, correlations in the power injections, and power flow physics, these fluctuations may cumulate so that line failures *emerge*, possibly triggering cascades.

This is highly relevant due to the increasing penetration of renewable energy sources in modern power grids and their susceptibility to weather conditions. This development poses several challenges to the design and control of such networks: intermittent and highly correlated power generation causes random fluctuations in the line power flows, possibly yielding outages and cascading failures. It is then of crucial importance to develop appropriate physical models that give fundamental insight.

The emerging nature of failures challenges the analysis. To tackle this, we use ideas from statistical physics and large deviations theory. We consider a stochastic model for the network power injections similar to that proposed in [28], introduce a positive real parameter ε describing the magnitude of the noise and focus on the *small-noise*

regime where $\varepsilon \rightarrow 0$. The parallel with statistical physics allows us to determine the most likely configuration of power injections that leads to failures and possibly cascades. Our results are explicit, and yield fundamental insights into the way cascades occur. Though we focus on a power grid, our approach is applicable to any network where fluctuations of the node inputs can trigger line failures.

We now give a detailed model description. Our network is represented by a connected graph G with n nodes representing the *buses* and m directed edges modeling the *transmission lines*. The stochastic fluctuations of the net power injections around their nominal values $\mu \in \mathbb{R}^n$ are modeled as a multivariate n -dimensional Gaussian random vector with mean μ

$$p \sim \mathcal{N}_n(\mu, \varepsilon \Sigma_p), \quad (1)$$

with the convention that p_i is the net power injected at node i . Differently for the usual assumption of the fluctuations being independent and identically distributed, we can allow for heterogeneous standard deviations of the power injections at the various nodes as well as for dependencies between of the fluctuations in different nodes by choosing a non-trivial covariance matrix Σ_p . This is instrumental, for instance, to model positive correlations due to geographical proximity of wind turbines and solar panels. Gaussianity is consistent with atmospheric physics [6, Section 1.7] and wind turbine statistics [4].

Assuming the mean power injection vector μ has zero sum and using the DC approximation [5, Chapter 4], the line power flows f are

$$f = Vp, \quad (2)$$

where V is a $m \times n$ matrix that encodes the power network topology and weights (modeling susceptances).

The assumption that the mean power injection vector μ has zero sum does not guarantee that the total net power injected in the network $\sum_{i=1}^n p_i$ is equal to zero as p is a random vector. This minor technical issue can be easily resolved by assuming that the total power injection mismatch is distributed uniformly among all the nodes

(we account for this in the matrix V , for details see the Supplemental Material).

In view of assumptions (1) and (2), the line power flows f also follow a multivariate Gaussian distribution, namely $f \sim \mathcal{N}_m(\nu, \varepsilon \Sigma_f)$. The vector $\nu = V\mu \in \mathbb{R}^m$ describes the average line flows, while the covariance matrix $\Sigma_f = V\Sigma_p V^T$ describes the correlations between line flows taking in account both by the correlations of the power injections (encoded by the matrix Σ_p) and those created by the network topology due to the physics of the power flows (Kirchhoff's laws) via the matrix V .

A line *overloads* if the absolute amount of power flowing in it exceeds a given *line threshold*. We assume that such an overload immediately leads to the outage of the corresponding line, to which we will henceforth refer simply as *line failure*. The failure of a line cause a global redistribution of the line power flows according to Kirchhoff's laws, which could trigger further failures and cascades.

Without loss of generality, we assume that the matrix V also contains information about the line thresholds, so that f is the vector of *normalized* line power flows and the failure of line ℓ is described by the event $\{|f_\ell| \geq 1\}$.

We consider a scenario where the power grid operates on average safely within the limits by assuming that $\max_{\ell=1, \dots, m} |\nu_\ell| < 1$ so that only large fluctuations of line flows lead to failures, which correspondingly become *rare events* as $\varepsilon \rightarrow 0$. To assess how much a network is "robust" against initiating failure and identify its most vulnerable lines, we derive the exponential decay of probabilities of single line failure events, namely $\{|f_\ell| \geq 1\}$ for $\ell = 1, \dots, m$. The theory of large deviations [27] is concerned precisely with calculating the exponential decay of rare events probabilities, which are usually referred to as *rate functions* or *entropy functions*. Since line flows have been normalized, we are interested in evaluating the rate function describing the failure event of any line ℓ in a single point, i.e. 1, and we refer to the corresponding value I_ℓ as *failure decay rate*. Thanks to the fact that the line power flow are Gaussian, we can explicitly calculate I_ℓ , see [27, Example 3.1], as

$$I_\ell = -\lim_{\varepsilon \rightarrow 0} \varepsilon \log \mathbb{P}_\varepsilon(|f_\ell| \geq 1) = \frac{(1 - |\nu_\ell|)^2}{2\sigma_\ell^2}, \quad (3)$$

where $\sigma_\ell^2 = (\Sigma_f)_{\ell, \ell}$ is the variance of the line flow f_ℓ . Thus, for small ε , we can approximate the probability of the emergent failure of line ℓ as

$$\mathbb{P}(|f_\ell| \geq 1) \approx \exp(-I_\ell/\varepsilon), \quad (4)$$

and that of the first emergent failure as

$$\mathbb{P}(\max_\ell |f_\ell| \geq 1) \approx \exp(-\min_\ell I_\ell/\varepsilon). \quad (5)$$

The decay rate I_ℓ depends on how close the (normalized) average power flow ν_ℓ is to the threshold 1 and

how large the variance σ_ℓ^2 is. Note that σ_ℓ^2 accounts for the power injections variability and correlations as well as for how much the network possibly amplifies or mitigates them. Decay rates can be used to identify lines that are most susceptible to the system's noise, as illustrated by Figure 1.

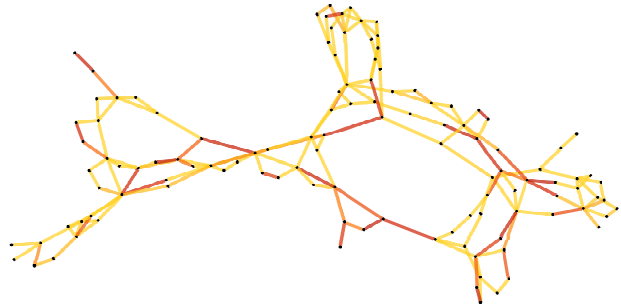


FIG. 1: Failure decay rates $\{I_\ell\}_{\ell=1, \dots, m}$ heat-map for the IEEE 118-bus test system. The likelihood of line failures is visualized using a color gradient in which the red lines are the most vulnerable ones.

Large deviations theory provides further analytic tools that give valuable insight in understanding the way a specific rare event occurs. Conditionally on the failure of line ℓ , the power injections configuration exhibits a sensible ("large") deviation from its mean that is characterized by

$$p^{(\ell)} = \arg \inf_{p \in \mathbb{R}^n : |e_\ell^T V p| \geq 1} \frac{1}{2} (p - \mu)^T \Sigma_p^{-1} (p - \mu). \quad (6)$$

Provided that $\nu_\ell \neq 0$, the solution is unique and reads

$$p^{(\ell)} = \mu + \frac{(\text{sign}(\nu_\ell) - \nu_\ell)}{\sigma_\ell^2} \sqrt{\Sigma_p} V^T e_\ell \in \mathbb{R}^n, \quad (7)$$

where $\text{sign}(a) = 1$ if $a \geq 0$ and -1 otherwise, while $e_\ell \in \mathbb{R}^m$ is the vector with the ℓ -th entry equal to 1 and zeros elsewhere (details in the Supplemental Material).

A key finding is that an emergent line failure does not occur due to large deviations in the power injections of the neighboring nodes, but as a cumulative effect of small unusual fluctuations of the power injections in the entire network "summed up" by power flow physics, see Figure 2.

Our approach allows to differentiate between different types of line failures: by calculating the line power flow profile $f^{(\ell)} := V p^{(\ell)}$ corresponding to the most likely power injections configuration leading to the failure of line ℓ , we can assess whether the most likely way for failure of line ℓ to occur is as

- an *isolated failure*, if $|f_k^{(\ell)}| < 1$ for any line $k \neq \ell$, or
- a *joint failure* of multiple lines together, if there exists some other line $k \neq \ell$ such that $|f_k^{(\ell)}| \geq 1$.

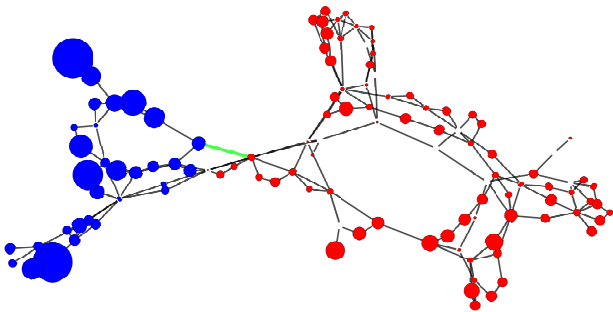


FIG. 2: Representation of the most likely power injections configuration of the IEEE 118-bus test system leading to the failure of the green line. Nodes size is adjusted proportionally to their deviations from their mean, while their color describes whether these deviations are positive (blue) or negative (red)

The resulting non-standard power injections configuration $p^{(\ell)}$ redistributes across an altered network $\tilde{G}^{(\ell)}$ (a subgraph of the original graph G) in which line ℓ (and possible other lines, in case of a joint failure) has been removed, possibly increasing the stress on the remaining lines. The way this redistribution happens on $\tilde{G}^{(\ell)}$ is governed by the power flow physics and we assume that it occurs instantaneously, without any transient effects. The power flow redistribution amounts to compute a new matrix \tilde{V} linking the power injections and the new power flows. The most likely power flow configuration on $\tilde{G}^{(\ell)}$ after redistribution is then $\tilde{f}^{(\ell)} = \tilde{V}p^{(\ell)}$.

In the special case of an isolated failure (say of line ℓ) it is enough to calculate only a vector $\phi^{(\ell)} \in \mathbb{R}^{m-1}$ of redistribution coefficients, known as *line overload distribution factors* (LODF) in power system engineering. Indeed, the most likely power flow configuration on $\tilde{G}^{(\ell)}$ after redistribution is equal to $\tilde{f}^{(\ell)} = (f_k^{(\ell)})_{k \neq \ell} \pm \phi^{(\ell)}$, where the sign of the second term depends to the direction in which the power flowed on line ℓ when the overload occurred.

The power flow configuration $\tilde{f}^{(\ell)}$ can be efficiently used to determine which lines will fail with high probability as a consequence of the original (possibly joint) failure, by checking for which line indices k we have $|\tilde{f}_k^{(\ell)}| \geq 1$, see the Supplemental Material for more details.

A rigorous probabilistic theory of emergent cascading failures can be developed by combining these two ingredients, the statistical physics results describing the most likely power injections configuration leading to the first failure and the power flow redistribution in the network afterwards. In particular, this approach explains several qualitative features of cascades in power grids that have been observed empirically, the most prominent one being the non-local propagation of failures.

We now illustrate how our framework can transparently explain this phenomenon using a ring network, in which there are exactly two paths along which the power can flow between any two nodes. Upon the failure of line ℓ , the power originally flowing on line ℓ must now

flow on the unique remaining path in the opposite direction. This observation can be made rigorous by showing that the redistribution coefficients are $\phi_k^{(\ell)} = -1$ for every $k \neq \ell$. It is intuitive that neighboring lines have positive correlated power flows, while distant lines have negative correlations as power flows must sum to zero by Kirchhoff's law. Hence, the most likely power injections configuration that makes the power flow in line ℓ exceeding the line threshold (say by becoming larger than 1) also makes the power flows in the antipodal half of the network negative. These will then go beyond the line threshold (by becoming smaller than -1) after the power flow redistributes, see Figure 3.

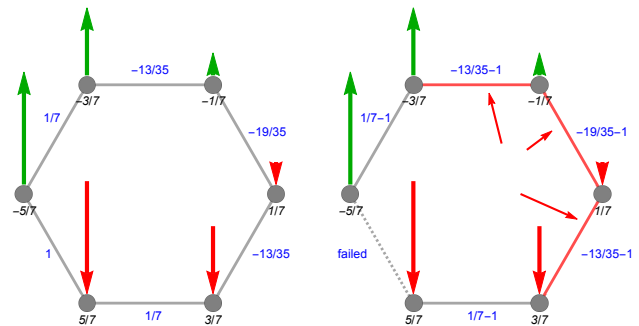


FIG. 3: On the left, the most likely power injections $p^{(\ell)}$ leading to the failure in black and power flows $f^{(\ell)}$ in blue. On the right, the situation after the power flow redistribution with three subsequent failures and the values of $\tilde{f}^{(\ell)} = (f_k^{(\ell)} - 1)_{k \neq \ell}$ in blue

Non-local failure propagation thus emerges from the interplay between the power flow configuration just before the line failure and the network structure, which determines the alternative paths along which power could flow after the line failure. Figure 4 shows an example of non-local failure propagation on a IEEE test system.

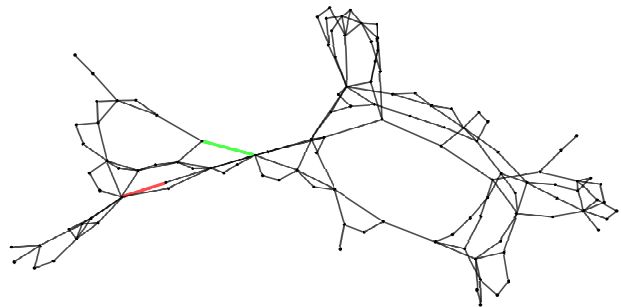


FIG. 4: The power injection configuration for the IEEE 118-bus test system that most likely causes the failure of green line after the power redistribution causes the red line to fail.

The most likely power injection configuration leading to the emergent failure of a given line can be used in combination with power flow redistribution routines to generate the failures triggered by that initial scenario. By repeating this procedure for all lines, one can obtain

Graph	% joint failures	$\mathbb{E}(F_1^{\text{ec}})$	$\mathbb{E}(F_2^{\text{ec}})$	$\mathbb{E}(F_2^{\text{cc}})$
IEEE14	65.0%	4.40	8.40	4.95
IEEE30	97.6%	3.73	9.88	4.95
IEEE39	80.4%	4.78	11.39	4.85
IEEE57	88.5%	8.00	19.00	10.44
IEEE96	72.2%	6.70	21.47	7.31
IEEE118	91.6%	10.40	24.53	7.56
IEEE300	87.0%	18.13	39.19	7.42

Table I: Percentage of joint failures in emergent cascades and average number of failed lines F_1 up to stage 1 and F_2 up to stage 2 for emergent cascades (ec) and classical cascades (cc) for some IEEE test systems.

insightful statistics of the first two stages of emergent cascading failures (ec) and compare them with those of classical cascading failures (cc), obtained using nominal power injection values rather than the most likely ones and deterministic removal of the initial failing line. For these numerical experiments, line thresholds are taken to be proportional to the average absolute power flow on the corresponding lines, i.e. $C_\ell = (1 + \alpha)|\nu_\ell|$ with $\alpha = 0.25$, and Σ_p to be the identity matrix.

As shown in Table I, emergent cascades have a very high percentage of joint failures and an average number of failures in the first cascade stage much larger than one (in classical cascades only one line is removed in the first cascade stage). Furthermore, the expected total number of failed lines up to the second cascade stage is significantly larger for emergent cascades than for classical cascades. Lastly, failures propagate in emergent cascades on average a bit less far than in classical cascades, as illustrated by the statistics of the failure jumping distance in Table II.

Graph	$\mathbb{E}(D^{\text{ec}})$	$\mathbb{E}(D^{\text{cc}})$	$c_v(D^{\text{ec}})$	$c_v(D^{\text{cc}})$
IEEE14	0.388	0.987	0.600	1.050
IEEE30	0.754	1.198	0.879	1.115
IEEE39	0.898	1.633	0.891	1.149
IEEE57	1.210	2.507	0.863	1.415
IEEE96	1.450	1.781	0.879	0.946
IEEE118	0.679	1.638	0.745	1.169
IEEE300	1.408	2.580	0.806	1.081

Table II: Average and coefficient of variation of the failure jumping distance D in stage 2 both for emergent cascades (ec) and classical cascades (cc). The distance between two lines is measured as the shortest path between any of their endpoints.

Our approach also gives a constructive way to build the so-called “influence graph” [14, 15, 22], in which a directed edge connects lines ℓ and ℓ' if the failure of the line ℓ triggers (simultaneously or after redistribution) that of line ℓ' . Figure 5 shows an example of influence graph

built using our large deviations approach. The *cliques* of the influence graph (i.e. its maximal fully connected subgraphs) can then be used to identify clusters of cosusceptible lines [34], which are the lines that statistically fail often in the same cascade event.

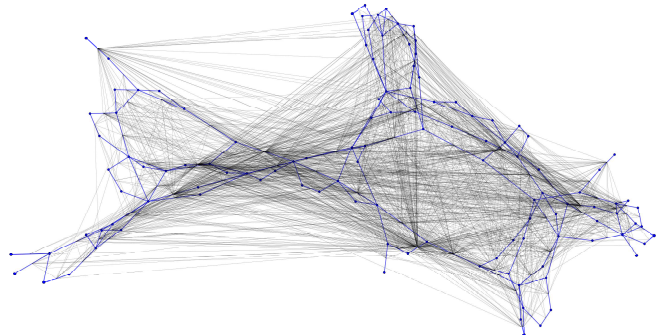


FIG. 5: The influence graph of the IEEE 118-bus test system (in black) built using the first two stages of all cascade realizations has a deeply different structure than the original network (in blue)

The proposed viewpoint on endogenous cascade failures can have important practical implications in terms of power system reliability: the most likely power injection configurations leading to (possibly joint) failures can be leveraged to improve the current $N - 1$ safety criterion which uses nominal values of power injection configurations.

-
- [1] R. Albert, I. Albert, and G. Nakarado. Structural vulnerability of the North American power grid. *Physical Review E*, 69(2):025103, feb 2004.
 - [2] R. Albert and A.-L. Barabási. Statistical mechanics of complex networks. *Reviews of Modern Physics*, 74(1):47–97, 2002.
 - [3] R. Albert, H. Jeong, and A.-L. Barabási. Error and attack tolerance of complex networks. *Nature*, 406(6794):378–382, jul 2000.
 - [4] J. Berg, A. Natarajan, J. Mann, and E. Patton. Gaussian vs non-Gaussian turbulence: impact on wind turbine loads. *Wind Energy*, 19(11):1975–1989, 2016.
 - [5] D. Bienstock. *Electrical Transmission System Cascades and Vulnerability*. SIAM, Philadelphia, dec 2015.
 - [6] D. Bienstock, M. Chertkov, and S. Harnett. Chance-Constrained Optimal Power Flow: Risk-Aware Network Control under Uncertainty. *SIAM Review*, 56(3):461–495, 2014.
 - [7] H. Cetinay, F. Kuipers, and P. Van Mieghem. A Topological Investigation of Power Flow. *IEEE Systems Journal*, pages 1–9, 2016.
 - [8] R. Cohen, K. Erez, D. Ben-Avraham, and S. Havlin. Resilience of the Internet to random breakdowns. *Physical Review Letters*, 85(21):4626–4628, 2000.
 - [9] R. Cohen, K. Erez, D. Ben-Avraham, and S. Havlin. Breakdown of the Internet under Intentional Attack.

- Physical Review Letters*, 86(16):3682–3685, apr 2001.
- [10] P. Crucitti, V. Latora, and M. Marchiori. Model for cascading failures in complex networks. *Physical Review E*, 69(4):045104, apr 2004.
- [11] P. Crucitti, V. Latora, M. Marchiori, and A. Rapisarda. Efficiency of scale-free networks: error and attack tolerance. *Physica A: Statistical Mechanics and its Applications*, 320:622–642, mar 2003.
- [12] I. Dobson, B. Carreras, V. Lynch, and D. Newman. Complex systems analysis of series of blackouts: Cascading failure, critical points, and self-organization. *Chaos: An Interdisciplinary Journal of Nonlinear Science*, 17(2):026103, jun 2007.
- [13] D. Heide, M. Schäfer, and M. Greiner. Robustness of networks against fluctuation-induced cascading failures. *Physical Review E*, 77(5):056103, may 2008.
- [14] P. Hines, I. Dobson, E. Cotilla-Sanchez, and M. Eppstein. "Dual Graph" and "Random Chemistry" Methods for Cascading Failure Analysis. In *2013 46th Hawaii International Conference on System Sciences*, pages 2141–2150. IEEE, jan 2013.
- [15] P. Hines, I. Dobson, and P. Rezaei. Cascading Power Outages Propagate Locally in an Influence Graph that is not the Actual Grid Topology. *IEEE Transactions on Power Systems*, 32(2):1–1, 2016.
- [16] R. Kinney, P. Crucitti, R. Albert, and V. Latora. Modeling cascading failures in the North American power grid. *European Physical Journal B*, 46(1):101–107, 2005.
- [17] B. Mirzsoleiman, M. Babaei, M. Jalili, and M. Safari. Cascaded failures in weighted networks. *Physical Review E*, 84(4):046114, oct 2011.
- [18] A. Motter. Cascade control and defense in complex networks. *Physical Review Letters*, 93(9):1–4, 2004.
- [19] A. Motter and Y.-C. Lai. Cascade-based attacks on complex networks. *Physical Review E*, 66(6):065102, 2002.
- [20] L. Powell. *Power system load flow analysis*. McGraw Hill, 2004.
- [21] K. Purchala, L. Meeus, D. Van Dommelen, and R. Belmans. Usefulness of DC power flow for active power flow analysis. In *IEEE Power Engineering Society General Meeting*, pages 2457–2462. IEEE, 2005.
- [22] J. Qi, K. Sun, and S. Mei. An Interaction Model for Simulation and Mitigation of Cascading Failures. *IEEE Transactions on Power Systems*, 30(2):804–819, mar 2015.
- [23] M. Schaub, J. Lehmann, S. Yaliraki, and M. Barahona. Structure of complex networks: Quantifying edge-to-edge relations by failure-induced flow redistribution. *Network Science*, 2(01):66–89, apr 2014.
- [24] S. Soltan, D. Mazaauric, and G. Zussman. Analysis of Failures in Power Grids. *IEEE Transactions on Control of Network Systems*, 4(2):288–300, jun 2017.
- [25] B. Stott, J. Jardim, and O. Alsac. DC Power Flow Revisited. *IEEE Transactions on Power Systems*, 24(3):1290–1300, 2009.
- [26] S. Sun, Z. Liu, Z. Chen, and Z. Yuan. Error and attack tolerance of evolving networks with local preferential attachment. *Physica A: Statistical Mechanics and its Applications*, 373:851–860, jan 2007.
- [27] H. Touchette. The large deviation approach to statistical mechanics. *Physics Reports*, 478(1-3):1–69, jul 2009.
- [28] Z. Wang, A. Scaglione, and R. Thomas. A Markov-Transition Model for Cascading Failures in Power Grids. In *2012 45th Hawaii International Conference on System Sciences*, pages 2115–2124. IEEE, jan 2012.
- [29] D. Watts. A simple model of global cascades on random networks. *Proceedings of the National Academy of Sciences*, 99(9):5766–5771, apr 2002.
- [30] D. Witthaut, M. Rohden, X. Zhang, S. Hallerberg, and M. Timme. Critical Links and Nonlocal Rerouting in Complex Supply Networks. *Physical Review Letters*, 116(13):138701, mar 2016.
- [31] D. Witthaut and M. Timme. Nonlocal failures in complex supply networks by single link additions. *The European Physical Journal B*, 86(9):377, sep 2013.
- [32] D. Witthaut and M. Timme. Nonlocal effects and countermeasures in cascading failures. *Physical Review E*, 92(3):032809, sep 2015.
- [33] A. Wood, B. Wollenberg, and G. Sheble. *Power generation, operation, and control*. John Wiley & Sons, 3rd edition, 2014.
- [34] Y. Yang, T. Nishikawa, and A. Motter. Vulnerability and Cosusceptibility Determine the Size of Network Cascades. *Physical Review Letters*, 118(4):048301, 2017.

SUPPLEMENTAL MATERIAL

Power grid model and DC approximation

We model the power grid network as a connected weighted graph G with n nodes, modeling buses, and m edges, representing the transmission lines. Choosing an arbitrary but fixed orientation of the transmission lines, the network structure is described by the *edge-vertex incidence matrix* $B \in \mathbb{R}^{m \times n}$ definite entry-wise as

$$B_{\ell,i} = \begin{cases} 1 & \text{if } \ell = (i, j), \\ -1 & \text{if } \ell = (j, i), \\ 0 & \text{otherwise.} \end{cases} \quad (8)$$

Denote by $\beta_\ell = \beta_{i,j} = \beta_{j,i} > 0$ the weight of edge $\ell = (i, j)$, corresponding to the *susceptance* of that transmission line. By convention, we set $\beta_{i,j} = \beta_{j,i} = 0$ if there is no transmission line between i and j . Denote by W the $m \times m$ diagonal matrix defined as $W := \text{diag}(\beta_1, \dots, \beta_m)$. The network topology and weights are simultaneously encoded in the *weighted Laplacian matrix* of the graph G , defined as $L := B^T W B$ or entry-wise as

$$L_{i,j} = \begin{cases} -\beta_{i,j} & \text{if } i \neq j, \\ \sum_{k \neq j} \beta_{i,k} & \text{if } i = j. \end{cases} \quad (9)$$

Denote by $J \in \mathbb{R}^{n \times n}$ the matrix with all entries equal to one. The relation between any vector of power injections $p \in \mathbb{R}^n$ and the phase angles $\theta \in \mathbb{R}^n$ they induce in the network nodes can be written in matrix form as

$$\theta = L^+ S p, \quad (10)$$

where $L^+ \in \mathbb{R}^{n \times n}$ is the *Moore-Penrose* pseudo-inverse of L and the matrix $S := I - \frac{1}{n} J \in \mathbb{R}^{n \times n}$ acts as a "global slack", ensuring that the net power injection is always

identically zero. Exploiting the eigenspace structure of L , L^+ can be calculated as

$$L^+ = \left(L + \frac{1}{n}J\right)^{-1} - \frac{1}{n}J, \quad (11)$$

In the literature, instead of L^+ it is commonly used another matrix \hat{L} , calculated using the inverse of the $(n-1) \times (n-1)$ sub-matrix obtained from L deleting the first row and first column the matrix L . In our method we are implicitly choosing an average value of zero as a reference for the nodes voltage phase angles, while in the classical one the first node is used as reference by setting its phase angle equal to zero. We remark that these two procedures are equivalent if one is interested in the line power flows, as these latter depend only on the phase angle differences.

We make use of the *DC approximation*, which is commonly used in high-voltage transmission system analysis [20, 21, 25, 33], according to which the real power flows \hat{f} are related with the phase angles θ via the linear relation $\hat{f} = B\theta$. In view of (10), the line power flow \hat{f} can be written as a linear transformation of the power injections p , i.e.

$$\hat{f} = WBL^+Sp. \quad (12)$$

It is convenient to look at the *normalized line power flow* vector $f \in \mathbb{R}^m$, defined component-wise as $f_\ell := \hat{f}_\ell/C_\ell$ for every $\ell = 1, \dots, m$, where C_ℓ is the *line threshold*, which we define using the nominal average power injection vector μ and choosing a tolerance parameter $\alpha > 0$ as

$$C_\ell = (1 + \alpha)|(WBL^+S\mu)_\ell|, \quad \ell = 1, \dots, m. \quad (13)$$

The relation between line power flows and normalized power flows can be rewritten as $f = Cf$, where C is the $m \times m$ diagonal matrix $C := \text{diag}(C_1^{-1}, \dots, C_m^{-1})$. In view of (12), the normalized power flows f can be expressed in terms of the power injections p as

$$f = Vp, \quad (14)$$

where $V := CWBL^+S \in \mathbb{R}^{m \times n}$.

Large deviation principles for failure events

In the following statement we write f_ε to stress the dependence of the line power flows on the noise parameter ε .

Proposition 1 *Assume that $\max_{j=1, \dots, m} |\nu_j| < 1$. Then, for every $\ell = 1, \dots, m$, the sequence of line power flows $(f_\varepsilon)_{\varepsilon > 0}$ satisfies the large deviations principle*

$$\lim_{\varepsilon \rightarrow 0} \varepsilon \log \mathbb{P}(|(f_\varepsilon)_\ell| \geq 1) = -\frac{(1 - |\nu_\ell|)^2}{2\sigma_\ell^2}. \quad (15)$$

The most likely power injection configuration $p^{(\ell)} \in \mathbb{R}^n$ given the event $\{|(f_\varepsilon)_\ell| \geq 1\}$ is the solution of the variational problem

$$p^{(\ell)} = \arg \inf_{p \in \mathbb{R}^n : |e_\ell^T V p| \geq 1} \frac{1}{2}(p - \mu)^T \Sigma_p^{-1} (p - \mu). \quad (16)$$

which, when $\nu_\ell \neq 0$, can be explicitly computed as

$$p^{(\ell)} = \mu + \frac{(\text{sign}(\nu_\ell) - \nu_\ell)}{\sigma_\ell^2} \sqrt{\Sigma_p} V^T e_\ell. \quad (17)$$

The line power flows corresponding to the power injection configuration $p^{(\ell)}$ can be calculated as

$$f^{(\ell)} = Vp^{(\ell)} = \nu + \frac{(\text{sign}(\nu_\ell) - \nu_\ell)}{\sigma_\ell^2} V \Sigma_p V^T e_\ell \in \mathbb{R}^m. \quad (18)$$

The vector $f^{(\ell)}$ can be also seen as the conditional expectation of random line power flow vector f_ε conditional on the failure event $\{f_\ell = \text{sign}(\nu_\ell)\}$, namely

$$f^{(\ell)} = \mathbb{E}[f_\varepsilon | (f_\varepsilon)_\ell = \text{sign}(\nu_\ell)], \quad (19)$$

and thus, in particular, for every $k = 1, \dots, m$

$$f_k^{(\ell)} = \nu_k + (\text{sign}(\nu_\ell) - \nu_\ell) \frac{\text{Cov}(f_\ell, f_k)}{\text{Var}(f_\ell)}. \quad (20)$$

Note that the case $\nu_\ell = 0$ has been excluded only for compactness. Indeed, in that case the variational problem (16) has two solutions, $p^{(\ell,+)}$ and $p^{(\ell,-)}$. This is easily explained as if the power flow on line ℓ has mean $\nu_\ell = 0$, then it is equally likely for the overload event $\{|f_\ell| \geq 1\}$ to occur as $\{f_\ell \geq 1\}$ or as $\{f_\ell \leq -1\}$ and the most likely power injection configurations that trigger them can be different.

The previous proposition immediately yields the large deviation principle also for the first line failure event $\{\|f_\varepsilon\|_\infty \geq 1\}$, which reads

$$\lim_{\varepsilon \rightarrow 0} \varepsilon \log \mathbb{P}(\|f_\varepsilon\|_\infty \geq 1) = -\min_{\ell=1, \dots, m} \frac{(1 - |\nu_\ell|)^2}{2\sigma_\ell^2}. \quad (21)$$

Indeed, the decay rate for the event that at least one line fails is equal to the minimum of the decay rates for the failure of each line. The most likely power injections configuration that leads to the event $\{\|f_\varepsilon\|_\infty \geq 1\}$ is $p^{(\ell^*)}$ with $\ell^* = \arg \min_{\ell=1, \dots, m} \frac{(1 - |\nu_\ell|)^2}{2\sigma_\ell^2}$.

Proof of Proposition 1.

Let $(Z^{(i)})_{i \in \mathbb{N}}$ be a sequence of i.i.d. multivariate normal vectors $Z^{(i)} \sim \mathcal{N}_m(\nu, \Sigma)$, and let $S_n := \frac{1}{n} \sum_{i=1}^n Z^{(i)}$ be the sequence of the partial sums. By setting $\varepsilon = \frac{1}{n}$, it immediately follows that that $f_\varepsilon \stackrel{d}{=} S_n$. Denote $g(p) :=$

$\frac{1}{2}(p - \mu)^T \Sigma_p^{-1} (p - \mu)$. Following [27, Section 3.D], we get

$$\begin{aligned} \lim_{\varepsilon \rightarrow 0} \varepsilon \log \mathbb{P}((f_\varepsilon)_\ell \geq 1) &= \lim_{n \rightarrow \infty} \frac{1}{n} \log \mathbb{P}((S_n)_\ell \geq 1) = \\ &= - \inf_{p \in \mathbb{R}^n : e_\ell^T V p \geq 1} g(p) = - \frac{(1 - \nu_\ell)^2}{2\sigma_\ell^2}, \end{aligned} \quad (22)$$

$$\begin{aligned} \lim_{\varepsilon \rightarrow 0} \varepsilon \log \mathbb{P}((f_\varepsilon)_\ell \leq -1) &= \lim_{n \rightarrow \infty} \frac{1}{n} \log \mathbb{P}((S_n)_\ell \leq -1) = \\ &= - \inf_{p \in \mathbb{R}^n : e_\ell^T V p \leq -1} g(p) = - \frac{(-1 - \nu_\ell)^2}{2\sigma_\ell^2}. \end{aligned} \quad (23)$$

The optimizers of problems (22) and (23) are easily computed respectively as as

$$\begin{aligned} p^{(\ell,+)} &= \mu + \frac{1 - \nu_\ell}{\sigma_\ell^2} \sqrt{\Sigma_p} V^T e_\ell, \\ p^{(\ell,-)} &= \mu + \frac{-1 - \nu_\ell}{\sigma_\ell^2} \sqrt{\Sigma_p} V^T e_\ell. \end{aligned}$$

Note that trivially

$$\begin{aligned} \inf_{p \in \mathbb{R}^n : |e_\ell^T V p| \geq 1} g(p) &= \\ &= \min \left\{ \inf_{p \in \mathbb{R}^n : e_\ell^T V p \geq 1} g(p), \inf_{p \in \mathbb{R}^n : e_\ell^T V p \leq -1} g(p) \right\}, \end{aligned}$$

and thus identities (15) and (16) immediately follow.

Power flow redistribution

For every line ℓ define $\mathcal{J}(\ell)$ to be the collection of lines that fail jointly with ℓ as

$$\mathcal{J}(\ell) := \{k : |f_k^{(\ell)}| \geq 1\}. \quad (24)$$

Let $j(\ell) = |\mathcal{J}(\ell)|$ its cardinality and note that $j(\ell) \geq 1$ as trivially ℓ always belongs to $\mathcal{J}(\ell)$. Denote by $\tilde{G}^{(\ell)}$ the graph obtained from G by removing all the lines in $\mathcal{J}(\ell)$.

Let us focus first on the case of the isolated failure of line ℓ , that is when $\mathcal{J}(\ell) = \{\ell\}$. In this case $\tilde{G}^{(\ell)} = G(V, E \setminus \{\ell\})$ is the graph obtained from G after removing the line $\ell = (i, j)$. Provided that the power injections remain unchanged, the power flows redistribute among the remaining lines. Using the concept of *resistance matrix* $R \in \mathbb{R}^{m \times m}$ and under the DC approximation, in [7, 23, 24] it is proven that alternative paths for the power to flow from node i to j exists (i.e. $\tilde{G}^{(\ell)}$ is still connected) if and only if $\beta_{i,j} R_{i,j} \neq 1$. In other words, $\beta_{i,j} R_{i,j} = 1$ can only occur in the scenario where line $\ell = (i, j)$ is a *bridge*, i.e. its removal results in the disconnection of the original graph G in two components. If $\tilde{G}^{(\ell)}$ is still a connected graph, the power flows after redistribution $\tilde{f}^{(\ell)} \in \mathbb{R}^{m-1}$ are related with the original line flows $f \in \mathbb{R}^m$ in the network G by the relation

$$\tilde{f}_k^{(\ell)} = f_k + \phi_{\ell,k} \text{sign}(\nu_\ell), \quad \text{for every } k \neq \ell, \quad (25)$$

where if $\ell = (i, j)$ and $k = (a, b)$ the coefficient $\phi_{\ell,k} \in \mathbb{R}$ can be computed as

$$\phi_{\ell,k} = \phi_{(i,j),(a,b)} := \beta_k \cdot \frac{C_\ell}{C_k} \cdot \frac{R_{a,j} - R_{a,i} + R_{b,i} - R_{b,j}}{2(1 - \beta_\ell R_{i,j})}, \quad (26)$$

It is easy to prove that in a ring network with homogeneous line thresholds and susceptances $\phi_{\ell,k} = -1$ for every $\ell \neq k$.

More in general (hence also in the case of joint failures), the most likely power flow configuration $\tilde{f}^{(\ell)}$ after redistribution in general can be written as

$$\tilde{f}^{(\ell)} = \tilde{V} p^{(\ell)}, \quad (27)$$

where the $(m-j(\ell)) \times n$ matrix \tilde{V} can be constructed analogously to V , but considering the altered graph $G^{(\ell)}$ instead of G . The next proposition shows that it is enough to look at the vector $\tilde{f}^{(\ell)}$ to determine whether a line that survived at the first cascade stage (i.e. that did not fail jointly with ℓ) will fail with high probability or not after the power redistribution (e.g. at the second cascade stage).

Proposition 2 For any $\delta \in (0, 1)$, define $Q_\delta^{(\ell)} := \{y \in \mathbb{R}^{m-j(\ell)} : |y_i| \leq 1 - \delta\}$. The following statement hold:

i) If $|\tilde{f}_k^{(\ell)}| < 1$ for any $k \notin J(\ell)$, then

$$\lim_{\varepsilon \rightarrow 0} \varepsilon \log \mathbb{P}(\tilde{f}_\varepsilon \notin Q_0^{(\ell)} \mid |(f_\varepsilon)_\ell| \geq 1) < 0; \quad (28)$$

ii) If there exists $k \notin J(\ell)$ such that $|\tilde{f}_k^{(\ell)}| \geq 1$, then

$$\lim_{\varepsilon \rightarrow 0} \varepsilon \log \mathbb{P}(\tilde{f}_\varepsilon \in Q_\delta^{(\ell)} \mid |(f_\varepsilon)_\ell| \geq 1) < 0. \quad (29)$$

Proof of Proposition 2. i) We have

$$\mathbb{P}(f_\varepsilon \notin \mathring{Q}^{(k)} \mid (f_\varepsilon)_\ell \geq 1) = \frac{\mathbb{P}(f_\varepsilon \notin \mathring{Q}^{(k)}, (f_\varepsilon)_\ell \geq 1)}{\mathbb{P}((f_\varepsilon)_\ell \geq 1)},$$

Denote $g(p) := \frac{1}{2}(p - \mu)^T \Sigma_p^{-1} (p - \mu)$. From large deviations theory it readily follows that

$$\lim_{\varepsilon \rightarrow 0} \varepsilon \log \mathbb{P}((f_\varepsilon)_\ell \geq 1) = - \inf_{p \in \mathbb{R}^n : e_\ell^T V p \geq 1} g(p) \quad (30)$$

$$\begin{aligned} \lim_{\varepsilon \rightarrow 0} \varepsilon \log \mathbb{P}(\tilde{f}_\varepsilon \notin \mathring{Q}_0^{(\ell)}, (f_\varepsilon)_\ell \geq 1) &= \\ &= - \inf_{\substack{p \in \mathbb{R}^n : e_\ell^T V p \geq 1, \\ \exists k \notin \mathcal{J}(\ell) : |e_k^T \tilde{V} p| \geq 1}} g(p). \end{aligned} \quad (31)$$

Define the corresponding decay rates as

$$I_\ell := \inf_{p \in \mathbb{R}^n : e_\ell^T V p \geq 1} g(p), \quad J_\ell := \inf_{\substack{p \in \mathbb{R}^n : e_\ell^T V p \geq 1, \\ \exists k \notin \mathcal{J}(\ell) : |e_k^T \tilde{V} p| \geq 1}} g(p). \quad (32)$$

Then we can rewrite

$$\lim_{\varepsilon \rightarrow 0} \varepsilon \log \mathbb{P}(\tilde{f}_\varepsilon \notin \mathring{Q}^{(k)} \mid (f_\varepsilon)_\ell \geq 1) = -J_\ell + I_\ell. \quad (33)$$

and, therefore,

$$\lim_{\varepsilon \rightarrow 0} \varepsilon \log \mathbb{P}(\tilde{f}_\varepsilon \notin \mathring{Q}^{(k)} \mid (f_\varepsilon)_\ell \geq 1) = 0 \iff J_\ell = I_\ell. \quad (34)$$

Notice that the feasible set of the minimization problem (31) is strictly contained in that of the problem (30), implying that $J_\ell \geq I_\ell$.

Recall that we denoted by $p^{(\ell)}$ the unique optimal solution of (30) and the corresponding line power flow vector $\tilde{f}^{(\ell)} = \tilde{V}p^{(\ell)}$. Let $\hat{p}^{(\ell)}$ be an optimal solution of (31) and

define $\hat{f}^{(\ell)} := \tilde{V}\hat{p}^{(\ell)}$. Clearly $\hat{p}^{(\ell)}$ is feasible also for problem (30). If it was the case that $J_\ell = I_\ell$, then $\hat{p}^{(\ell)}$ would be an optimal solution also for (30), and thus by uniqueness ($g(p)$ is strictly convex) $\hat{p}^{(\ell)} = p^{(\ell)}$ and $\hat{f}^{(\ell)} = \tilde{f}^{(\ell)}$. But this leads to a contradiction, since by assumption $|\tilde{f}_k^{(\ell)}| < 1$ for all $k \notin \mathcal{J}(\ell)$, while $\hat{f}^{(\ell)}$ is by construction such that there exists $k \notin \mathcal{J}(\ell)$ such that $|\hat{f}_k^{(\ell)}| \geq 1$. Hence $J_\ell > I_\ell$ and we conclude that

$$\lim_{\varepsilon \rightarrow 0} \varepsilon \log \mathbb{P}(\tilde{f}_\varepsilon \notin \mathring{Q}^{(k)} \mid (f_\varepsilon)_\ell \geq 1) < 0. \quad (35)$$

The proof in the case $(f_\varepsilon)_\ell \leq -1$ is analogous and so is that of statement (ii).